



HAL
open science

Environmental disturbances of trophic interactions and their impacts on a multi-host sapronotic pathogen

Ahmadou Sylla, Christine Chevillon, Magdalene Dogbe, Kayla M. Fast, Jennifer Pechal, Alex Rakestraw, Matthew E Scott, Michael W Sandel, Heather Jordan, M Eric Benbow, et al.

► **To cite this version:**

Ahmadou Sylla, Christine Chevillon, Magdalene Dogbe, Kayla M. Fast, Jennifer Pechal, et al.. Environmental disturbances of trophic interactions and their impacts on a multi-host sapronotic pathogen. 2024. hal-04563160

HAL Id: hal-04563160

<https://hal.science/hal-04563160>

Preprint submitted on 29 Apr 2024

HAL is a multi-disciplinary open access archive for the deposit and dissemination of scientific research documents, whether they are published or not. The documents may come from teaching and research institutions in France or abroad, or from public or private research centers.

L'archive ouverte pluridisciplinaire **HAL**, est destinée au dépôt et à la diffusion de documents scientifiques de niveau recherche, publiés ou non, émanant des établissements d'enseignement et de recherche français ou étrangers, des laboratoires publics ou privés.



Distributed under a Creative Commons Public Domain Mark 4.0 International License

Environmental disturbances of trophic interactions and their impacts on a multi-host sapronotic pathogen

Ahmadou Sylla^{1,2,3,4*}, Christine Chevillon¹, Magdalene Dogbe⁵, Kayla M. Fast⁶, Jennifer L. Pechal⁴, Alex Rakestraw⁴, Matthew E. Scott⁶, Michael W. Sandel^{6,7}, Heather Jordan⁵, M. Eric Benbow^{4,8,9,10}, Jean-François Guégan^{1,2,3}

¹ MIVEGEC, Université de Montpellier (UM), Centre National de la Recherche Scientifique (CNRS), Institut de Recherche pour le Développement (IRD), Institut national de recherche pour l'agriculture, l'alimentation et l'environnement (INRAE), Montpellier, France,

² Epidémiologie des maladies animales et zoonotiques (UMR EPIA), Université Clermont Auvergne, INRAE, VetAgro Sup, Saint-Genès-Champanelle, France

³ Epidémiologie des maladies animales et zoonotiques (UMR EPIA), Université de Lyon, INRAE, VetAgro Sup, Marcy l'Etoile, France

⁴ Department of Entomology, Michigan State University, East Lansing, MI, USA

⁵ Department of Biological Sciences, Mississippi State University, MS, USA

⁶ Department of Wildlife, Fisheries, and Aquaculture, Mississippi State University, MS, USA

⁷ Fish and Wildlife Research Center, Mississippi State University, MS, USA

⁸ Department of Osteopathic Medical Specialties, Michigan State University, East Lansing, MI, USA, ⁹ Ecology, Evolution and Behavior Program, Michigan State University, East Lansing, MI, USA

¹⁰ AgBioResearch, Michigan State University, East Lansing, MI, USA

*Corresponding authors

Correspondence: nando2014@hotmail.fr (AS)

Authors' ORCID :

A. Sylla: 0009 0008 3111 0604

C. Chevillon: 0000-0002-1262-5839

M. Dogbe: 0000-0003-1533-6095

K.M. Fast: 0000-0001-5476-5330

J. Pechal: 0000-0002-2588-2519

A. Rakestraw: 0000-0002-8087-0780

M.W. Sandel: 0000-0001-9083-9202

H. Jordan: 0000-0002-4197-2194

M.E. Benbow: 0000-0003-2630-0282

J.-F. Guégan: 0000-0002-7218-107X

ABSTRACT

Sapronotic pathogens are constituents of complex trophic networks, such as those that structure aquatic and soil ecosystems. In such habitats, sapronotic pathogens live and reproduce among microbial consortia, and occasionally infect hosts and cause sapronotic disease (sapronosis). Sapronotic pathogens include almost all fungal microparasites and about a third of the bacterial pathogens infecting humans, including for instance non-tuberculous mycobacteria. Even though sapronotic agents are naturally present in the environment, their population dynamics are unknown. Despite growing rates of sapronotic disease incidence among humans and other animals, very few studies have examined sapronotic transmission and dynamics in the context of spatially explicit trophic networks. Patterns of sapronotic pathogen transmission arise from complex interactions,

51 including pathogen natural history, non-host and host environments, and spatial and temporal scales of the
52 system. In order to infer and ultimately predict how environmental disturbances affect trophic interactions and
53 influence sapronotic ecology, we analyzed host and non-host species interacting as prey and as micro- and
54 macropredators within a metacommunity context. Using a set of differential equation models, we assessed
55 responses of environmental load dynamics of a sapronotic disease agent, i.e., a mycobacterial pathogen, within a
56 general framework of environmental disturbance. We show that variation in top-down and horizontal
57 interactions mediated sapronotic pathogen abundance and dynamics in the environment. Our findings indicate
58 that habitat change and trophic interactions within host-pathogen relationships may strongly affect sapronotic
59 pathogen ecology through both synergistic and opposing mechanisms. This work provides for the first time an
60 understanding of environmental disturbance consequences on trophic webs that include major sapronotic
61 pathogens. In addition, the results provide a basis for interpreting the development of epidemics and epizootics
62 in the context of ecosystem modifications, particularly that of agriculture. Further research of this type will
63 provide a better understanding of the complex dynamics of sapronotic pathogens in animals and humans
64 responding to global change.

65
66
67 **Keywords:** Infectious disease, sapronosis, environmental pathogen, trophic interactions, environmental
68 disturbances, mathematical modeling, disease ecology

70 Human activities often cause environmental disturbances that affect biodiversity patterns across spatial
71 scales (Dornelas et al., 2014). Characterizing how this may affect infectious disease risks has been challenging,
72 notably because of the complexity of ecological interactions among biodiversity levels, ecosystem functioning
73 and the transmission strategies that pathogens have evolved for persisting in time and space (Rohr *et al.* 2020).
74 Also, pathogen transmission patterns arise from complex interactions of local transmission and the broader
75 spatial and temporal scales of the system (Lanzas et al. 2020). Indeed, disease pathogens, by altering life-history
76 traits of infected hosts, affect the relations between biodiversity and ecosystem functioning (Frainer *et al.* 2018).
77 Reciprocally, studies have shown predator top-down control effects on parasite infection patterns (Clarke et al.
78 2019). In analyzing environmental transmission of pathogens, linking host and non-host environment, and
79 pathogen scales can be particularly challenging; and this can be made even more complex by taking into account
80 human ecosystem disturbances. Trophic interactions are important to ecosystem functioning, energy transfer
81 and biodiversity maintenance, and environmental disturbance can strongly impact trophic interactions in
82 communities (Cuff et al. 2023). With environmental disturbances predicted to become increasingly more
83 important, it is urgent to understand how changes may affect particular functional guild of communities and
84 consequently influence spatial and temporal dynamics of environmental pathogen ecology (Ostfeld et al. 2008).
85 Unfortunately, there is little disease ecology modeling work showing how environmental disturbances affecting
86 particular trophic guilds can cascade into infectious disease transmission dynamics. This type of ecosystem-based
87 research is crucial to more broadly understanding the effects of local to global environmental changes on animal
88 and human health (Johnson et al. 2015). Most scientific research, both empirical and theoretical, has focused on
89 understanding the ways disease pathogens affect the existing inter-relationships in food webs, or on studying
90 changes in food-web properties, i.e., modifying nodes and links, and their consequences in disease agents
91 (Lafferty et al. 2008, Selakovic et al. 2014). Other work has looked at the effects of pathogens on food webs by
92 studying the impact on the demography of a particular trophic level (De Rossi et al. 2014). In general, the
93 theoretical analysis of the cascading effects of environmental disturbances acting on trophic webs and impacting
94 on the presence and population dynamics of an environmentally-borne pathogen, not affecting trophic layers but
95 having consequences for riverine species and even humans, has not been carried out (Ostfeld et al. 2008,
96 Rossberg 2013).

97 Among infectious disease agents, sapronotic pathogens form an important group constituted by fungi,
98 protozoa and bacteria that can cause opportunistic infections in wild and domestic animals and humans through
99 inhalation, ingestion and open wounds and trauma. They infect animal or human hosts by opportunity, and at
100 least one third of human bacterial diseases are caused by sapronoses (Kuris, Lafferty and Sokolow 2014). Non-
101 host environments such as freshwater, soils, decaying organic matter and abiotic or biotic surfaces are important
102 components of the lifecycle of many sapronotic pathogens (Receveur et al. 2022). These environments provide
103 microhabitats in which sapronotic microbes may replicate or survive, facilitating transmission and persistence in
104 time and space (Garchitorena et al. 2015a,b). Expanding human habitat use and landscape change of natural
105 ecosystems presents emerging opportunities for animal and human sapronotic pathogens (Guerra et al. 2021).

106 *Mycobacterium ulcerans* (MU), the causative agent of Buruli ulcer (BU), a skin neglected tropical disease, is a
107 sapronotic pathogen (Lanzas et al. 2020) that has drawn considerable attention by disease ecologists during the
108 last decade (see Douine et al. 2017, Receveur et al. 2022 for review). Environmental disturbances, notably those
109 of human origins (e.g., deforestation, mining, dam construction, agricultural development), are known to be
110 associated with increased BU disease risks in humans (Merritt *et al.* 2010, Guégan *et al.* 2020). Recent evidence
111 indicates MU presence in aquatic habitats, e.g., soil, water column, macrophyte substrates, and in a wide
112 diversity of aquatic and riverine macroorganisms, depending on seasonal periodicity (Garchitorena et al. 2015b,
113 Morris et al. 2016a,b, Receveur et al. 2022). Since the MU DNA concentration in the water column is generally
114 low due to the volume of water required for filtration, research has usually inferred MU presence and dynamics

115 from patterns in MU carriage among aquatic macroorganisms (Garchitorena et al. 2015b, Receveur et al. 2022).
116 Widely diverse taxa up to 80-90 different taxonomic orders (e.g., fishes, annelids, mollusks, aquatic and
117 terrestrial arthropods) naturally carry MU without necessarily promoting disease symptoms (Morris et al. 2016b,
118 Receveur et al. 2022). Time-series analyses assessing seasonal variations in the distribution and carriage of MU
119 among these aquatic and riverine species also showed that direct acquisition of MU from contaminated water
120 bodies in Central Africa was the main mode of transmission to humans compared to alternative routes
121 (Garchitorena et al. 2015a). Depending on weather conditions throughout the year, specifically increased rainfall
122 patterns, MU load has been shown to increase in aquatic environments, having consequences on transmission
123 risk to humans that occupy those areas (Garchitorena et al. 2015a).

124 In the present work, we focus on the MU sapronotic disease agent using a metapopulation approach and
125 differential equations modeling to model host-parasitic dynamics the role of trophic chains and environmental
126 disturbances on sapronotic disease ecology. Taking advantage of recent work on MU ecology and dynamics in
127 aquatic ecosystems (Garchitorena et al. 2015a,b), we first explore the role of trophic levels on the persistence
128 and population dynamics of this sapronotic system. We then analyze the effects of local and regional
129 environmental disturbances on trophic chains and their cascading effects on MU distribution in aquatic
130 ecosystems. We provide a theoretical framework through which other types of sapronotic systems can be
131 analysed and used in a predictive manner in the assessment of environmental disturbance on natural ecosystems
132 and their biodiversity. By understanding how disturbance impacts disease dynamics in ecological networks, we
133 argue for more research on sapronotic disease agents in wild and domestic animals, and humans. We finally call
134 for an explicit focus on developing mathematical modeling of sapronoses given their relative incidence and
135 importance in animal and public health.

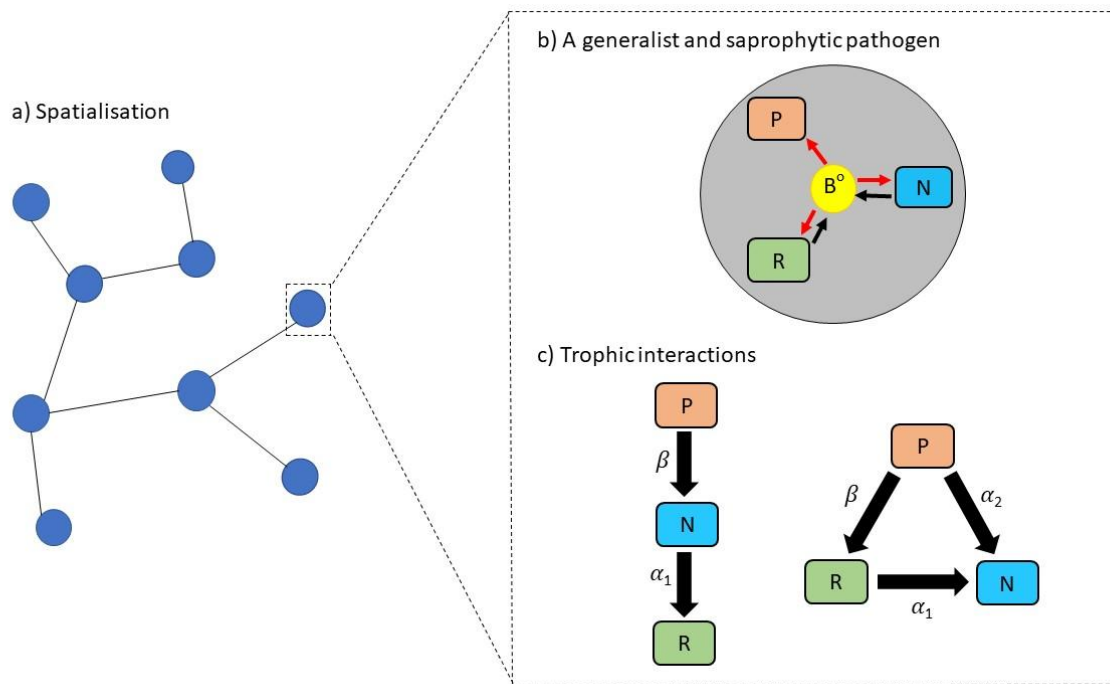
136

137

Materials and Methods

138 Model formulation

139 We propose a spatially explicit metacommunity model where a generalist and saprophytic bacterial
140 pathogen, e.g., *M. ulcerans*, coexists and interacts with three functional groups of free-living species: prey,
141 representing excellent habitats for pathogen survival and reproduction, and two groups of predators, hereafter
142 referred to as micro- and macropredators. Figure 1 illustrates the interspecific interactions considered. Table 1
143 details the functions and parameters of the metacommunity model. Although micropredators exclusively feed
144 on prey, we consider two scenarii depending on macropredator diet. The first is a simple trophic chain, with
145 macropredators feeding on micropredators that in turn consume preys. The second, called intraguild predation
146 (Arim and Marquet 2004), stipulates that micro- and macro-predators may share a common resource: under
147 that scenario, macropredators are generalist feeding on both preys and micropredators with the diet changing
148 when micropredators become locally rare. Trophic interactions allow pathogen transmission from infected
149 species to their predators. We incorporated the fact that the pathogen is a saprophytic bacterium by considering
150 its population dynamics as a free-living saprophyte and by explicitly formulating the exchanges between the
151 environmental saprophytic state and infectious states. Free-living bacterial cells may directly attach to living
152 organism surfaces (called biomass hereafter), and then can be released from infected organisms upon death
153 (hereafter refer to as bacterial saprophytic transmission). Bacterial doubling times and carrying capacity of
154 biomass-associated bacteria differed between the three functional groups (Table 1). We modeled a
155 metacommunity model with nine different local patches differing in productivity level, i.e., in the nutrients
156 available for prey survival and growth. We integrated this heterogeneity in the model by conserving among-
157 patches differences in prey growth rate (r_i) and carrying capacity (K_i).



158

159
 160
 161
 162
 163
 164
 165
 166
 167
 168
 169
 170
 171
 172
 173
 174
 175
 176

Figure 1. Schematic representation. State variables and parameters are defined in Table 1. Panel a illustrates the metacommunity in space: it includes nine habitat patches (represented by blue dots) that differ in productivity levels and are interconnected (connections represented by black lines), which allows macropredator migration across patches. Panels b and c describe the interspecific interactions occurring within each local patch as illustrated on panel a. Panel b focuses on the characteristics of a bacterial pathogen that is both generalist and saprophytic, hence occurring within patches as both free-living bacteria (B^0) and in association with different organisms (i.e., P, N and R for macropredators, micropredators and prey, respectively). The red and black arrows respectively represent the attachment rates of free-living bacteria to living biomass and the releases of free-living bacteria from dead infected organisms when their bodies are decomposing. Panel c shows scenarios of trophic interactions considered depending on the diet of the macropredators when micropredators are only feeding on prey. Macropredators can be specialists feeding only on micropredators (on the left) or generalists feeding on micropredators and prey (on the right). We defined α_1 and α_2 as parameters describing the attack rates onto prey by micro- and macropredators, respectively, and by β the attack rate of macropredators onto micropredators. This allowed switching from the trophic chain scenario, illustrated on the left, to the intraguild predation scenario, figured on the right, simply by manipulating the value taken by α_2 (null on the left and non-null on the right).

177
178
179
180

Table 1. Functions and parameters of the metacommunity model. The third column indicates the values taken by default for the different parameters across experiments. When no value is illustrated, it means that parameter is either a vector or a function, and its value is specified in section 2.2.

Notations	Descriptions	Values
State functions		
N_i	Density of prey species in patch i	
R_i	Density of micropredator species in patch i	
P_i	Density of macropredator species in patch i	
B_i^N	Density of prey-associated bacteria in patch i	
B_i^R	Density of micropredator-associated bacteria in patch i	
B_i^P	Density of macropredator-associated bacteria in patch i	
B_i^o	Density of free-living bacteria in patch i	
Parameters		
r_i	Intrinsic growth rate of prey species in patch i	-
K_i	Environmental carrying capacity of preys in patch i	1
μ	Natural mortality of preys	0.05
α_1	Maximal attack rate of micropredators onto preys	0.4
α_2	Maximal attack rate of macropredators onto preys	0 or 0.25
β	Maximal attack rate of macropredators onto micropredators	0.25 or 0.5
e_1, e_2, e_3	Constants of the Beddington–DeAngelis functional response	0.1
b	Constant of the Beddington–DeAngelis functional response	1
h	Constant of the Beddington–DeAngelis functional response	1
C_1	Food conversion efficiency of preys into micropredator births	0.7
C_2	Food conversion efficiency of preys into macropredator births	0.7
C_3	Food conversion efficiency of micropredators into macropredator births	0.7
d_1	Natural death rate of micropredators	0.05
d_2	Natural death rate of macropredators	0.05
$m_i(t)$	Migration rate of macropredator in patch i	-
q_{ji}	Probability that an individual from patch i migrates to patch j	1/8
ξ	Bacterial attachment rate on prey biomass	0.4
γ	Bacterial attachment rate on micropredator biomass	0.13
ρ	Bacterial attachment rate on macropredator biomass	0.06
s_N	Half-saturation constant of prey-associated substrate	1
s_1	Half-saturation constant of micropredator-associated substrate	1
s_2	Half-saturation constant of macropredator-associated substrate	1
θ	Growth rate of prey-associated bacteria	0.05
θ	Growth rate of micropredator-associated bacteria	0.02
θ_1	Natural mortality of prey-associated bacteria	0.03
θ_2	Natural mortality rate of micropredator-associated bacteria	0.2
$\Lambda(t)$	Natural mortality rate of macropredator-associated bacteria	0.3
δ	Time-dependence free-living bacteria growth rate	-
κ	Natural mortality rate of free-living bacteria	0.03
σ	Bacilli release rate from decomposing bodies of infected preys	3
	Bacilli release rate from decomposing bodies of infected micropredators	2

181 In patch i , we denoted by functions of time t : N_i the density of prey, R_i the density of micropredator species,
182 P_i the density of macropredator species, B_i^N the density of prey-associated bacteria, B_i^R the density of
183 micropredator-associated bacteria, B_i^P the density of macropredator-associated bacteria, and by B_i^o the density
184 of free-living bacteria in the aquatic environment. We assume that the prey population obeys a classical logistic
185 growth, with r_i referring to the intrinsic growth rate and K_i to the environmental carrying capacity. Due to
186 predation, the prey population size decreases by a quantity proportional to prey and predator populations. Here,
187 the predator-prey interactions are modeled via Beddington–DeAngelis’ functional response (Beddington 1975,
188 DeAngelis *et al.* 1975). This functional response is an enhancement of the well-known Holling’s type II functional
189 response including a term representing interference among predators. Increasing the density of consumers (i.e.,
190 predators) also reduces the consumption rate of the resource (i.e., preys). Several studies in the ecological
191 literature have considered this type of response (Cantrell *et al.* 2004, Ghanbari and Kumar 2019, Ji and Wang
192 2022, Tripathi *et al.* 2015).

193 Using the functions and parameters described in Table 1, we formulated the model as follows. The dynamics
 194 of biomass for the three functional groups in patch i are given by:

$$\frac{dN_i}{dt} = r_i N_i \left(1 - \frac{N_i}{K_i}\right) - \mu N_i - \frac{(\alpha_1 R_i + \alpha_2 P_i) N_i}{1 + e_1 R_i + e_2 P_i + b N_i} \quad (1)$$

$$\frac{dR_i}{dt} = \frac{c_1 \alpha_1 R_i N_i}{1 + e_1 R_i + e_2 P_i + b N_i} - d_1 R_i - \frac{\beta P_i R_i}{1 + e_3 P_i + h R_i} \quad (2)$$

$$\frac{dP_i}{dt} = \frac{c_2 \alpha_2 P_i N_i}{1 + e_1 R_i + e_2 P_i + b N_i} - d_2 P_i + \frac{c_3 \beta P_i R_i}{1 + e_3 P_i + h R_i} - m_i P_i + \sum_{j \neq i} m_j q_{ij} P_j \quad (3)$$

195

196 Parameters α_1 and α_2 denote, respectively, the attack rate of micro- and macropredators onto preys.
 197 Parameter β represents the predation rate of macropredators onto micropredators. Predator growth clearly
 198 depends on food consumption. We thus define c_1 , c_2 and c_3 as the respective food conversion efficiency of
 199 predators, representing thus the number of newborn predators resulting from their consumption. In absence of
 200 prey, micro- and macropredator densities decay exponentially at rate d_1 and d_2 , respectively. The term μN_i
 201 describes the prey loss due to natural mortality. Our model also incorporates macropredator migration events
 202 across the different local communities. At each time t , a fraction of macropredators $m_i(t)$ leaves patch i to other
 203 patches. A part q_{ji} of these emigrants choose patch j as destination. Thus, the flux of biomass from patch i to
 204 patch j at time t is $m_i(t) q_{ji} P_i(t)$. Summing the immigrants coming from all the other patches to patch i provides
 205 the last term figuring in equation (3).

206 The dynamics of prey-associated, micropredator-associated and macropredator-associated bacteria in patch i
 207 are respectively given by:

$$\frac{dB_i^N}{dt} = \frac{\xi N_i B_i^o}{s_N + N_i} + \frac{\theta N_i}{s_N + N_i} B_i^N - (\eta + \mu) B_i^N - \frac{(\alpha_1 R_i + \alpha_2 P_i) B_i^N}{1 + e_1 R_i + e_2 P_i + b B_i^N} \quad (4)$$

$$\frac{dB_i^R}{dt} = \frac{\gamma_i R_i B_i^o}{s_1 + R_i} + \frac{\lambda R_i B_i^R}{s_1 + R_i} - (\nu_1 + d_1) B_i^R + \frac{\alpha_1 R_i B_i^N}{1 + e_1 R_i + e_2 P_i + b B_i^N} - \frac{\beta P_i B_i^R}{1 + e_3 P_i + h B_i^R} \quad (5)$$

$$\frac{dB_i^P}{dt} = \frac{\rho P_i B_i^o}{s_2 + P_i} - (\nu_2 + d_2) B_i^P + \frac{\alpha_2 P_i B_i^N}{1 + e_1 R_i + e_2 P_i + b B_i^N} + \frac{\beta P_i B_i^R}{1 + e_3 P_i + h B_i^R} - m_i B_i^P + \sum_{j \neq i} m_j q_{ij} B_j^P \quad (6)$$

208

209 The intrinsic growth rate of host-associated bacteria depends upon the density of predators and prey
 210 biomasses as substrates for bacterial development. The parameters η , ν_1 and ν_2 correspond, respectively, to the
 211 natural mortality rate of prey-associated, micropredator-associated and macropredator-associated bacteria. Here,
 212 we used Michaelis-Menten' type functional response to describe bacilli attachment to biomass, which is
 213 proportional to both population biomass and free-living bacteria densities. We defined the maximum success
 214 rates for bacilli attachment on prey, micropredators and macropredators as ξ , γ_i and ρ , respectively. The
 215 biomass-associated bacteria are able to replicate on alive biomass until surface saturation concentration is
 216 reached. Focusing for instance on prey-associated bacteria, the Michaelis-Menten' type functional response is
 217 thus given by $\theta N_i / (N_i + s_N)$, where θ is the maximum production rate of prey-associated bacteria, and s_N is the
 218 half-saturation constant in this type of micro-habitat. The same functional response was used for predator-
 219 associated bacterial reproduction. Saprophytic bacilli growing on the surface of living biomass are released when
 220 the bodies of dead infected organisms are decomposing, which thus produce free-living bacteria (Godfray *et al.*
 221 1999, Kunttu *et al.* 2009, Merikanto *et al.* 2018). These phenomena, assumed to occur only in prey-and
 222 micropredator guilds (i.e., macropredators are considered dead-ends for the pathogen), are here described by

223 parameters κ and σ . Note that, aside such releases, biomass mortality reduces the concentration of biomass-
 224 associated bacteria that are respectively described by terms $-\mu B_i^N$, $-d_1 B_i^R$ and $-d_2 B_i^P$ in equations (4), (5) and (6),
 225 respectively. Similarly, while feeding on the prey present in patch i , predators locally decrease the number of
 226 prey-associated bacteria. In our model, we further incorporated the changes in the local densities of biomass-
 227 associated bacteria resulting from migration of macropredators among connected patches (see above).

228 The dynamics of free-living bacteria in patch i is given by:

$$\frac{dB_i^o}{dt} = (\Lambda - \delta)B_i^o - \frac{\xi N_i B_i^o}{s_N + N_i} - \frac{\gamma_i R_i B_i^o}{s_1 + R_i} - \frac{\rho P_i B_i^o}{s_2 + P_i} + \kappa \mu B_i^N + \sigma d_1 B_i^R \quad (7)$$

229 where $\Lambda(t)$ and δ are the reproduction and natural mortality rates of free-living bacteria, respectively. The
 230 body decomposition of infected organisms, either preys or micropredators, release saprophytic bacteria in the
 231 environment, increasing thus the local density in free-living bacteria in the patch when these organisms died (see
 232 terms $\kappa \mu B_i^N$ and $\sigma d_1 B_i^R$ in equation (7)).
 233

234 The metacommunity dynamics result from macropredators dispersal among-patches. We considered this
 235 dispersal to be active, depending on the local availability of resources. In the trophic chain scenario (Figure 1c,
 236 left), we have described the migration rate, $m_i(t)$, as a function inversely proportional to the local density of
 237 micropredators:

$$m_i(t) = \frac{u}{1 + R_i(t)} \quad (8)$$

238 where u is the maximal dispersal rate. In the alternative scenario considering macropredators as generalists
 239 (Figure 1c, right), we have described the migration rate, $m_i(t)$, as a function inversely proportional to both local
 240 densities of prey and micropredators:
 241

$$m_i(t) = \frac{u}{1 + R_i(t) + N_i(t)} \quad (9)$$

242 These definitions ensure that the migration rate of macropredators will increase when local food abundance
 243 decreases. For simplicity, we suppose that the pool of emigrants leaving the patch i has equal probability to
 244 reach any other local habitats ($q_{ij}=1/(n-1)$).
 245

246 Regarding environmental disturbances, we focused on cases where they promote sudden increases in preda-
 247 tor mortality, hence instantaneous decreases in predator densities (P_i and/or R_i). We also considered perturba-
 248 tions that, in addition to their sudden and direct impact on predator mortality, reduce the growth rate in preys,
 249 r_i , relatively to the value determined by the primary productivity level of the affected patch (see below, the third
 250 simulating experiment). Given differences among simulation experiments considered in the present paper, the
 251 modeling methodology is further developed within each section referring to a particular experiment.

252 Simulation parameters

253 We simulated a metacommunity composed of nine interconnected local sites. We set the vector describing
 254 prey growth rate among sites as $r = [0.15, 0.17, 0.2, 0.23, 0.25, 0.28, 0.31, 0.35, 0.38]$. We simulated free-living
 255 bacteria reproduction as simple Weibull's distribution ($t = 4 \times \text{Weibull}(t, 100, 4)$). Table 1 presents the values taken
 256 by default across all simulations by other parameters. We conducted numerical analysis of the model using the
 257 MATLAB software (MATLAB, ver. 8.6).

258 Results

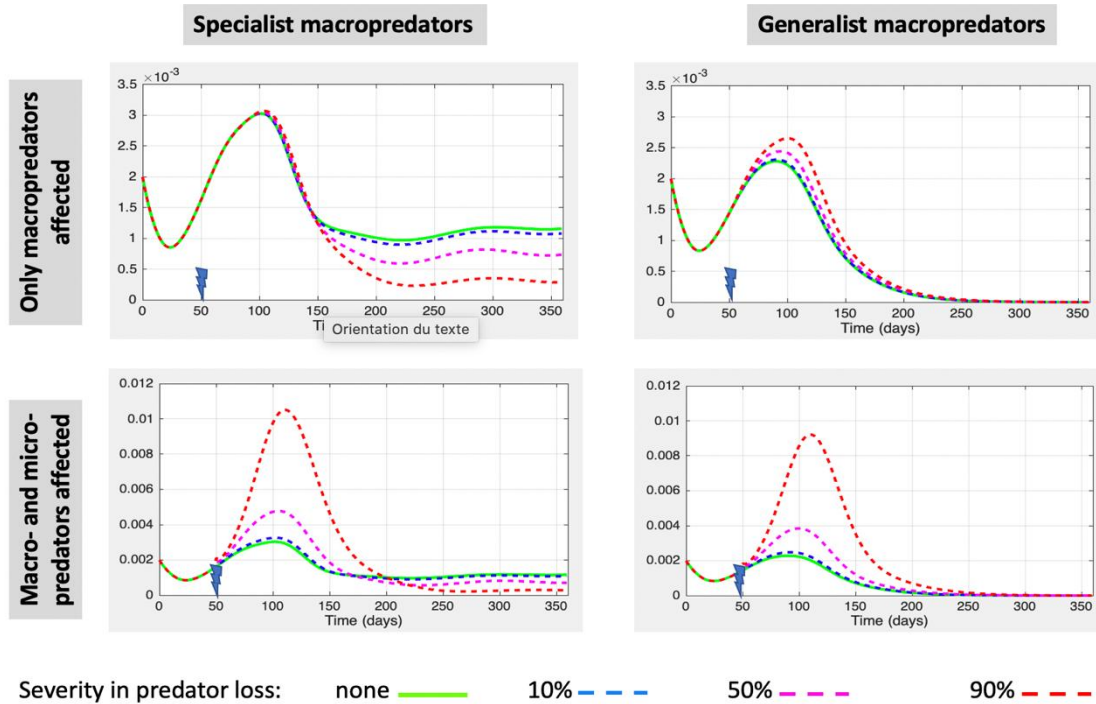
259 Numerical simulations are proposed with the aim of understanding how disturbing local communities affects,
260 via their direct and indirect impacts on species communities, the infection risks by a bacterial pathogen that is
261 both generalist and saprophytic. For each model scenario, we randomly chose the timing of disturbances, and
262 repeated simulations with different starting dates of disturbances and variable severity impacts on local
263 communities. We explored the properties of the model by investigating how such variations in timing, spatial
264 scale and/or severity of disturbances affect free-living bacteria density. For each model scenario, we run the
265 simulations long enough for encompassing the two phases that follow the occurrences of perturbations; i.e., a
266 first phase along which the food web remains destabilized, and a second where it reaches a new dynamic
267 equilibrium. In the two first experiments, local or regional environmental perturbations are instantaneous events
268 that only affect predatory guilds: predator densities in disturbed patch(es) are recovering just after the
269 environmental disturbance as function of the local resources. In the third experiment, environmental
270 disturbances reduce the densities of predator but also affects prey growth, with this latter effect lasting for
271 several days or weeks, promoting delays in both prey and predator recoveries relatively to expectations for
272 undisturbed habitats. Hereafter, for the sake of brevity, we have selected the most interesting and informative
273 findings.

274 **Experiment 1: Local ecological disturbance (i.e., affecting a single patch)**

275

276 The Figure 2 illustrates cases of local environmental disturbance that occurs when the fluctuating density in
277 saprophytic bacteria was naturally rising. For a same species assemblage at $t = 0$, four possibilities exist. The
278 environmental disturbance may affect only macropredators (Fig. 2, top panels) or both macro- and
279 micropredators (Fig. 2, bottom panels). Macropredators may be specialist (left panels) or generalist (right panels).
280 In each panel, the green curve represents the temporal dynamics in free-living bacteria density that one would
281 have observed in absence of disturbance. Green curves are thus identical in the two right panels (left panels,
282 respectively) but obviously different between left and right panels. Other lines represent the dynamics in free-
283 living density observed after disturbance.

284 In all panels, the most obvious impact of disturbance onto the dynamics in free-living bacteria density relies
285 to the period along which the local food-web remains destabilized. There is a temporary increase in sapronotic
286 bacteria along that period, which results from a temporary excess of the inputs from the decomposing bodies of
287 previously infected organisms relatively to the observations in absence of disturbance. For a given food-web
288 structure (i.e., for panels within the same column in Figure 2), such an excess is much higher when the
289 disturbance affects both predatory guilds, enriching thus the community in unconsumed preys (bottom panels)
290 relatively to the case where disturbance only affect macropredators (top panels). For a given impact of
291 disturbance (i.e., for panels within the same raw), the food-web structure matters on the long-term response to
292 local disturbance. Indeed, in trophic chain scenarios (i.e., involving only specialist predators), the post-
293 disturbance equilibrium translates in a reduction in free-living bacteria density relatively to the pre-disturbance
294 equilibrium. This is not the case for food webs involving generalist macropredators: there, the pre- and post-
295 disturbance equilibria of the system result in similar dynamics in free-living bacteria density.



296

297

298

299

300

301

302

303

Figure 2: Effects of local disturbances onto the local dynamics in free-living bacteria density. X-axes represent time and Y-axes free-living bacteria density. In all panels, green curves represent the local density in free-living bacteria in absence of perturbation. Other curves refer to the dynamics in free-living bacteria for an instantaneous reduction in predator densities at $t = 50$, when disturbance occurs, ranging from 10% to 90%. The perturbations affect only macropredators in top panels but both micro- and macropredators in bottom panels. Macropredators are specialists in left panels and generalists in right ones. Predation parameters used in trophic chain scenarios are $\alpha_2 = 0$ and $\beta = 0.5$; they are $\alpha_2 = 0.25$ and $\beta = 0.25$ otherwise.

304

Experiment 2: Regional ecological disturbance affecting predators

305

306

307

308

309

310

311

Here, we consider the case of regional ecological disturbance so that (i) every patch is the subject of local disturbance once a year and (ii) within-patches disturbances evenly affect micro- and macropredators. Patches still differ from one another in primary productivity (hence in prey logistic growth). Local disturbances can occur as synchronous events across all patches or as asynchronous events that include time lags between disturbances affecting distinct patches. In addition, disturbances may differ in the severity of predator reductions they induced. We thus simulated synchronous and asynchronous events with homogeneous (i.e., all local communities suffer the same reduction in both micro- and macropredator densities) and heterogeneous effects across patches.

312

313

314

315

Figure 3 shows the simulation results obtained for specialist macropredators. Panels a-d are evidence of the importance of time lags between successive disturbances affecting distinct patches with homogenous severity. Specifically, synchronous events (panel a) or short delays (panel c) between successive disturbances events lead to larger temporary increases in regional average in free-living bacteria density.

316

317

318

319

320

321

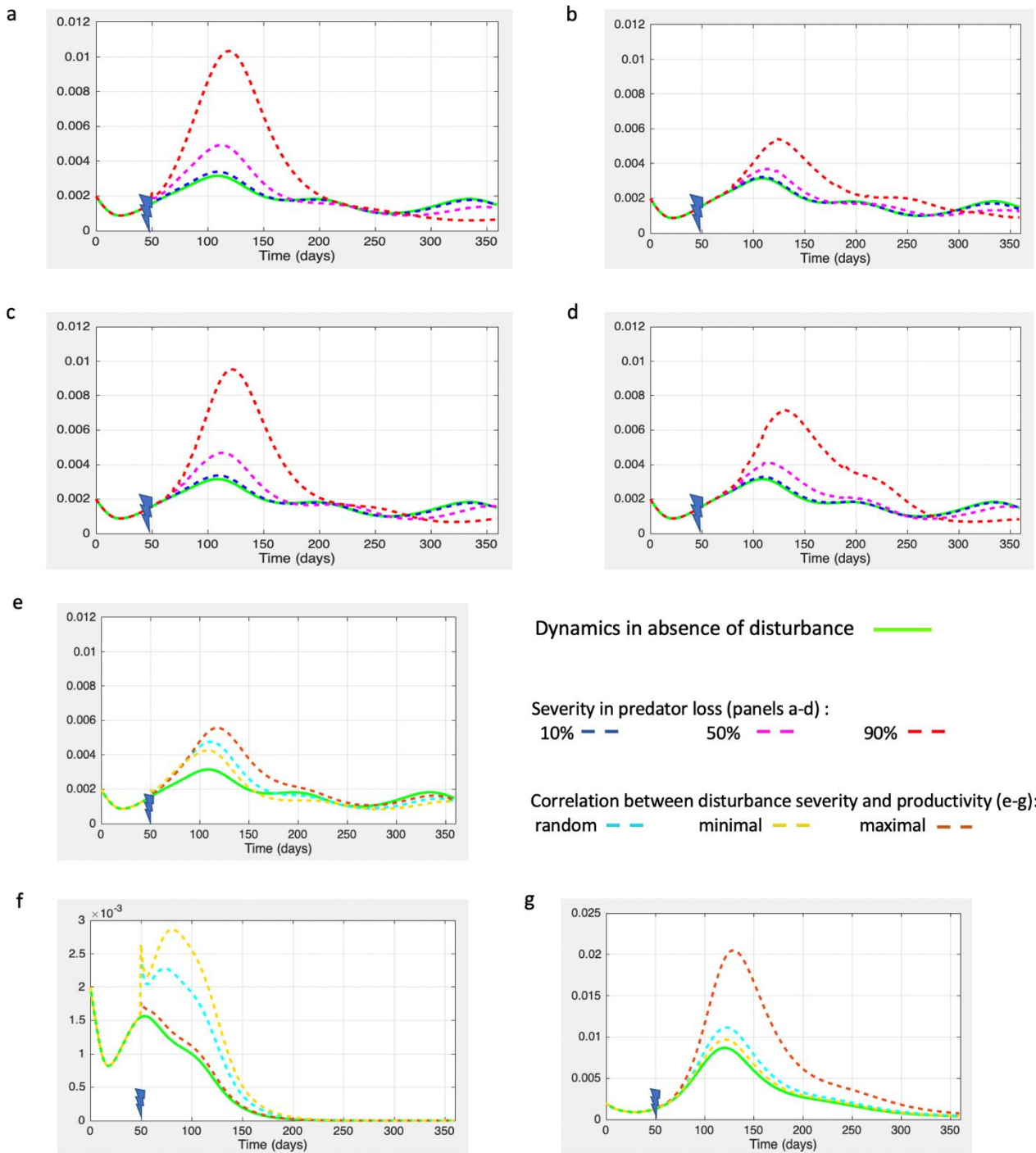
322

323

324

Next, we assessed the importance of heterogeneity in predator losses resulting from synchronous regional disturbance on free-living bacteria density. Here, there are two sources of heterogeneity among patches: differences in primary productivity r (ranging from 0.15 to 0.38) and differences in predator losses (randomly selected from 0% to 100%). In order to examine the interplay between the two sources of heterogeneity, we explored the dynamics in the regional average in free-living bacteria density when the correlation between them was random, minimal or maximal (Figure 3, panel e-f). At local scale, the impact of the heterogeneity in disturbance severity exceeds that of the heterogeneity in productivity (see the yellow curve in f panel and/or the red curve in g panel). Unsurprisingly, at the regional scale, the highest rebound in free-living bacteria density occurs when the correlation between both sources of among-patches heterogeneity is maximal (Figure 3e).

325 Results obtained for generalist macropredators are similar and presented in supplementary materials (Figure
326 S1). It is nevertheless noteworthy that, as previously observed at local scale (Figure 2), the diet of the
327 macropredators affects the long-term response of the metapopulation to a succession of local disturbances. On
328 the one hand, when both predator guilds are specialist, the main difference between pre- and post-disturbances
329 equilibria at metapopulation scale translates into a reduction in in free-living bacteria density (Figure 3). On the
330 other hand, when macropredator are generalist, the long-term response of the metapopulation to a succession
331 of local disturbances tend to be the same as that observed in absence of disturbance (Figure S1).



332

333

334

335

336

337

338

339

340

341

342

343

344

345

346

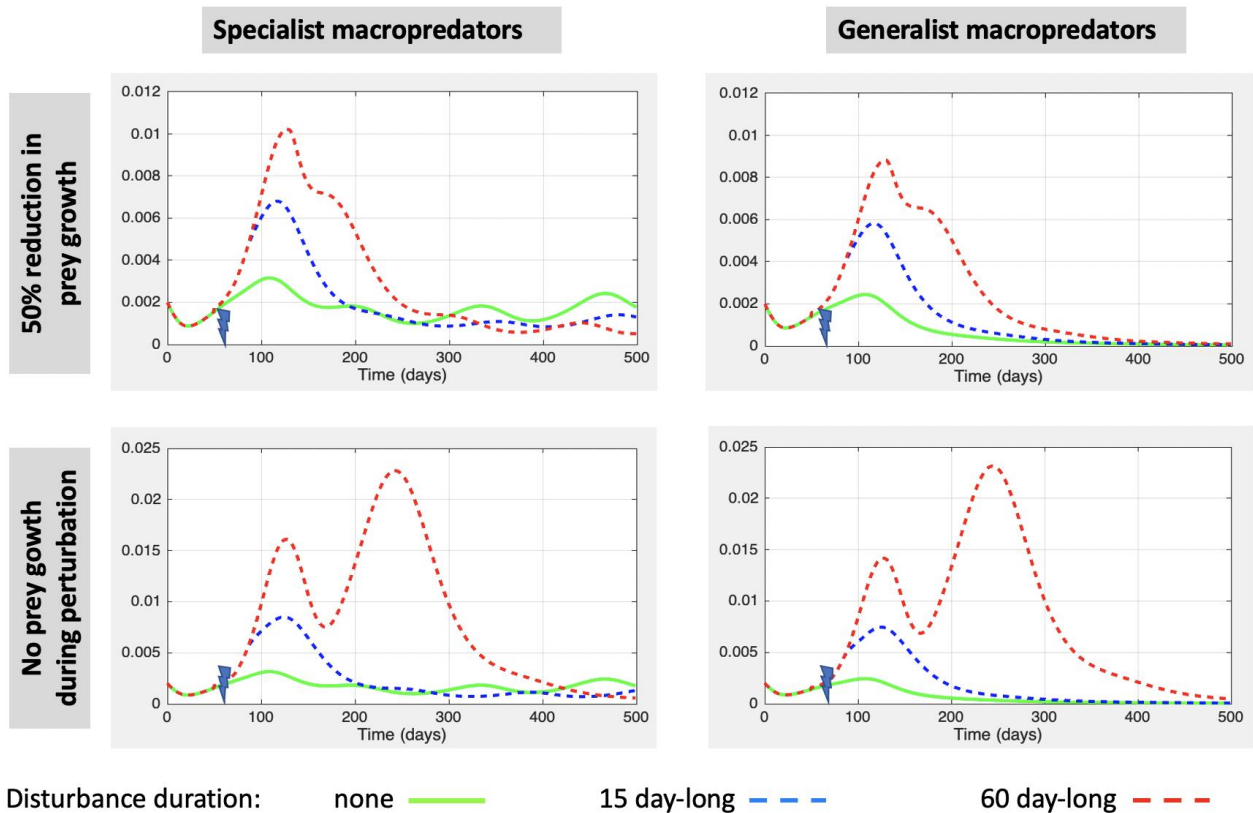
Experiment 3: Regional ecological disturbance also affecting preys

Figure 3. Impact of a succession of within-patches disturbances (trophic chain scenario). The diet of specialist macropredators is described by $\alpha_2 = 0$ and $\beta = 0.5$. First local disturbance occurs at $t = 50$ days. Panels a-e consider the regional scale of the entire metapopulation. Green curves refer to the regional dynamics in free-living density observed in absence of disturbances and others to those observed after successions of within-patches disturbances. In a-d panels, all local disturbances have homogeneous impact on within-patches predator densities. These local events are synchronized across patches in panel a. In panel b, the vector describing random timing of local disturbances across patches is $t = [50, 123, 180, 346, 50, 211, 81, 271, 92, 183]$. Time lags between successive disturbances last 5 and 20 days in panels c and d, respectively. In panel e, local disturbances are synchronized events with heterogeneous impacts on predator densities across patches. Panels f and g focus on the within-patches responses observed in the least and most productive patches, respectively.

347

348 The results presented so far concern disturbance with instantaneous effects that only affect predator guilds.
349 However, some perturbations, such as pollution resulting from gold mining, may affect all species present in
350 aquatic ecosystems. Here, we explore cases where disturbances affect all functional groups although differently.
351 Disturbances instantaneously reduce predator densities, but promote a temporary or lasting reduction in prey
352 population growth.

353 We carried out a sensitivity analysis on the duration of the blockage period of prey growth after disturbance
354 for different impacts of local reproduction rate r_i . Figure 4 shows the results of simulations in cases where r_i
355 is reduced either by 50% (top panels) or by 100% (bottom panels), and where macropredators are either specialist
356 (left panels) or generalist (right panels). We found that the regional average in free-living bacterial density
357 depends on how long and to which extent disturbances affects prey growth. It is noteworthy that the extent in
358 the reduction in prey growth (here, 50% versus 100%) have larger impacts on metapopulation responses
359 relatively to the period duration of such effects on prey (here, 15 days versus 60 days).



360

Disturbance duration: none — 15 day-long - - - 60 day-long - - -

361

362

363

364

365

366

367

368

369

370

371

372

Figure 4. Regional disturbance effects on prey and predators that impact density of free-living bacteria over the metacommunity. X-axes represent time; disturbances occur at $t = 69$ days. Y-axes refer to the regional averages in free-living bacteria density. Macropredators are specialist ($\alpha_2 = 0$ and $\beta = 0.5$) in left panels and generalist ($\alpha_2 = 0.25$ and $\beta = 0.25$) in right panels. Green curves refer to the regional average dynamics in saprophyte density observed in absence of disturbances. Those are identical in both left panels (right panels, respectively) but differ between right and left panels. Disturbances promote instantaneous reductions in predators. The vector describing the heterogeneity across patches in predator losses is [0.6663, 0.5391, 0.6981, 0.6665, 0.1781, 0.1280, 0.9991, 0.1711, 0.0326]. The blue and red curves refer to the regional responses in free-living bacteria density to disturbances blocking prey growth for 15 and 60 days, respectively. The reduction in prey growth during disturbances is 50% and 100% in top and bottom panels, respectively. Please note that the scale of the Y-axes in bottom panels exceeds those referring to regional average in bacterial loads in Figures 2 and 3.

373 **Experiment 4: Relaxing dispersal constraints on functional groups including species competent for the**
374 **pathogen survival and growth**

The first three experiments focused on cases where macropredators, which are dead-end hosts for the bacterial pathogen, constitute the only functional ecological group that include species dispersing across the metacommunity. We tested the dependency of the results withdrawn under this hypothesis by re-computing simulations for each experiment while assuming that species from the three trophic levels disperse across the metacommunity (everything else remaining unchanged). We assumed passive and non-oriented dispersal for preys, so that a fixed percentage of preys emigrate from each local site and evenly distribute among the other local sites. For micropredators, we assumed active migration that depends on the local resources in preys (i.e., obeying to the same rules than those defined for specialist macropredators; see equation #8 above).

375 Figures S3-S6 detail results for experiments 1-3 under two dispersal hypotheses for preys and micropredators
376 (cases A and B). In case A, we fixed prey dispersal at 1% and maximal dispersal rates of micro- and macro-
377 predators at 5% and 70%, respectively. In case B, we fixed prey dispersal at 6% and maximal dispersal rates of
378 micro- and macropredators at 10% and 70% for micro- and macropredators, respectively. Comparing those to
379 figures 2-3 and S1 evidence that the signals observed when only macropredator disperse remain if species from
380 all functional groups disperse. Introducing dispersal of prey and micropredator nonetheless tend to make
381 perturbations promoting lower and delayed peaks in the abundance of free-living bacteria relatively to cases
382 where only macropredator disperse.

383 **Discussion**

384 Empirical studies show that predators affect animal and human pathogen emergence and spread, even though
385 they reduce prey and vector abundances (Cohen *et al.* 1990). Despite evidence that interactions among
386 predators, prey and other species might affect environmental pathogen abundance, few empirical or modeling
387 studies have examined such interactions in a food-web context (see Clark *et al.* 2019). This is problematic since a
388 better assessment of multitrophic interactions affecting pathogen dynamics in complex species communities
389 could greatly increase our understanding of disease ecology. Here, we assessed, using a mathematical approach,
390 how local and regional disturbances of micropredator - macropredator - prey trophic interactions affect the
391 environmental load of a saprotoxic and generalist pathogen, i.e., *Mycobacterium ulcerans* causing cutaneous
392 infections in animals and humans, and responsible for Buruli ulcer in humans. Interestingly, our models are
393 sufficiently flexible and adaptable to other types of saprotoxic and generalist pathogens, assuming some basic
394 modifications of equations (e.g., suppression of the parasite life cycle).

395 Our study shows that interactive effects of the aquatic environment and multi-host and non-host local
396 communities affected over space and time the abundance of an environmental pathogen under a range of sce-
397 narios. Notably, the effects of environmental disturbances were strongly context-dependent and had differential
398 effects on the population dynamics of the environmental pathogen, and thus on potential transmissibility to
399 animals and humans. In this system, we found that the magnitude of predator effects on prey abundance, which
400 impacted environmental pathogen prevalence, were considerably stronger when both micro- and
401 macropredators were affected by local and regional environmental disturbance regimes. In general, the role of
402 disease pathogens and parasites in ecological webs is critical in shaping communities of populations (Dobson *et*
403 *al.* 2008). Based on these considerations, then, in this work we wanted to consider the influence of environmen-
404 tal perturbations on a food system composed of three trophic levels, and their effects on population dynamics of
405 a saprotoxic disease agent. We assumed that the disease did not affect any trophic levels in the food web, but
406 impacted on terrestrial animals and humans, using the example of *Mycobacterium ulcerans*, a neglected tropical
407 skin disease in human. Several modeling studies exist that analysed the effect of pathogens on di-trophic sys-
408 tems, e.g., phytoplankton species and grazers (Beltrami and Carroll 1994, see also Rossi *et al.* 2014), and many

409 others have empirically studied the prey-predator interactions and their impacts on parasite population dynam-
410 ics (Tian and Stenseth 2019 for hantavirus disease, Levi et al. 2012 for Lyme disease as two illustrative examples;
411 see Ostfeld et al. 2008 for a more general overview). In this work, we were interested in considering disease
412 agents in a larger ecosystem, namely a trophic chain composed of three trophic layers, and mathematically ana-
413 lyse the impacts of environmental disturbance on prey-predator-pathogen relationships. At least to our
414 knowledge, this is the first time that a research work is identifying how habitat perturbation impacts the identity
415 and frequency of a disease agent through mediated effects on trophic interactions.

416 First, our results demonstrate that, in a situation of local disturbance, density and diet regime, i.e.,
417 specialist *versus* generalist, are important factors in driving top-down effects of macropredators on
418 environmental pathogen population dynamics. This effect is much greater when macropredators are specialised
419 on feeding upon a particular micropredator species (Figure 2, top left panel) than when being generalists (Figure
420 2, top right panel). In fact, specific predation on a micropredator species leads to a relaxation of the pressure
421 exerted on prey, and therefore leads to an increase in their abundance in the environment, and thus, providing
422 favorable ecological conditions for sapronotic agents (Figure 2, top left panel). However, when macropredators
423 are generalists, the consequences on the pathogen are less important due to a dual effect of intraguild
424 competition. In this situation, there is a threshold effect of macropredator density on environmental pathogen
425 abundance (Figure 2, top right row) depending on both macropredator diet strategy and local species diversity. In
426 a situation where the local environmental disturbance affects both micro- and macropredator compartments,
427 there is a significant impact on the population dynamics of the bacteria, whatever the type of macropredator
428 diet. However, the increase in environmental pathogen abundance is slightly greater when macropredators are
429 generalists. These results are consistent with studies showing top-down effects of local environmental
430 disturbances on plant vector-borne pathogen dynamics through consumptive and non-consumptive effects
431 (Finke 2012, Clarke *et al.* 2019).

432 Second, regional environmental disturbances affect local food-webs through both micro- and
433 macropredator guilds, where synchronous or high-frequency disturbance events lead to higher pathogen
434 abundance in the environment (Figure 3a-d). In addition, disturbance severity is more important to pathogen
435 load than local biomass productivity and spatial heterogeneity (Figure 3e). We also found that regional
436 disturbance did not influence how predator diet regime, i.e., generalist or specialist, affected pathogen dynamics
437 (Figure S1).

438 Third, in the case of more extreme environmental disturbance in which prey guilds are also affected, we
439 observed that local food-web effects on pathogen dynamics were mediated by impacts on prey population
440 growth (Figure 4). Also, stronger impacts were observed for important reduction in prey reproduction rate rela-
441 tively to perturbation duration, which did not significantly affect pathogen load.

442 Our modeling work has focused on analyzing the dynamic behavior of a sapronotic agent over a period
443 of one year, for which we currently have sufficient empirical knowledge. Based on the knowledge gradually ac-
444 quired, it will be necessary to study their complex and non-linear dynamics over multi-decadal time steps, which
445 are more in tune with the tempo of local and more global changes currently taking place all over the planet.

446 Our theoretical study supports recent reviews and models that posit food-web theory provides im-
447 portant insights to understanding direct and indirect effects of ecological interactions involving disturbances,
448 environmental heterogeneity and multi-host dynamics on pathogen transmission and disease ecology (Roche *et al.*
449 2013, Seabloom *et al.* 2015, Crowder *et al.* 2019). Notably, at local scales the strength and magnitude of dis-
450 turbance on macropredators mediated the population dynamics of environmental pathogens in the case of spe-
451 cialized macropredators only. More broadly, regional environmental perturbations may affect pathogen dynam-
452 ics when severe, long-term or successive disturbance events occur in a short period of time. This simulation
453 study that integrates multitrophic frameworks to assess human (or other animal)-biodiversity-environmental
454 pathogen communities will help us better understand and interpret why epidemics or epizootics of environmen-
455 tal pathogens can suddenly develop and spread. Further, it can promote better control and management of
456 these harmful animal and human infectious diseases.

457

458 **Conclusion**

459

460 Since zoonotic disease agents have one or multiple reservoir hosts in the environment, their control is
461 rendered impossible or ineffective if this origin is not taken into account. Control of such animal and human
462 diseases therefore requires a thorough understanding of the host-parasite dynamics and pathogen ecology in
463 their environment, which is very rarely the case. Zoonotic diseases may become a problem for wild and
464 domestic animals, e.g., livestock, and humans when exposure increases or spillovers to other animal species of
465 human concern, e.g., contacts between wildlife and livestock, happen. Models of zoonotic pathogen
466 transmission are extremely rare in the current scientific literature. Our modeling study shows that zoonoses
467 may be highly dependent on the environmental conditions prevailing in species communities, and regulated by
468 prey-predator relationships in trophic chains. In addition, these zoonoses are themselves highly sensitive to
469 local and large-scale environmental disturbances impacting species communities in a cascade of effects' process.
470 It is important for human and veterinary medicine, but also more generally, to recognize that the control of these
471 zoonoses requires a better understanding of their ecology and environmental dynamics. Too few
472 epidemiological studies have examined the influence of environmental change and species community structure
473 on disease transmission, and this should constitute a priority for subsequent investigation. Mathematical
474 modeling, combined with new experimental studies, represents a highly valuable tool to better understand
475 environmental transmitted pathogens and their population biology, and to project possible scenarios for future
476 zoonotic outbreaks in the current international context of global change.
477

478

Acknowledgements

479 The authors are particularly grateful to INRAE, IRD, CNRS, Université de Montpellier, Michigan State
480 University and Mississippi State University for their support.

481

Funding

482 The authors are supported by two "Investissement d'Avenir" grants from the Agence Nationale de la
483 Recherche (CEBA ANR-10-LABX-2501 and CEMEB ANR-10-LABX-0401). All authors are supported by the joint
484 NSF-NIH-NIFA Ecology and Evolution of Infectious Disease program [DEB 1911457]. AS received a postdoctoral
485 fellowship from DEB 1911457 and MEB received a visiting professor fellowship from LabEx CEMEB.

486

Conflict of interest disclosure

487 Any opinions, findings, conclusions, or recommendations expressed in this publication are those of the
488 authors and do not necessarily reflect the view of the institutions and funding agencies quoted above. The
489 authors declare that they comply with the PCI rule of having no financial conflicts of interest in relation to the
490 content of the article.

491

Scripts, code, and supplementary information availability

492 Script and codes are available online (<https://doi.org/10.5281/zenodo.11085318>; Sylla et al., 2024a);
493 Supplementary figures are available online (<https://zenodo.org/records/11083413>; Sylla et al. 2024b).

494

References

495 Arim M., Marquet P.A. (2004). Intraguild predation: a widespread interaction related to species biology. *Ecology*
496 *Letters*, 7, 557-564. <https://doi.org/10.1111/j.1461-0248.2004.00613.x>

497 Beddington J. (1975). Mutual interference between parasites or predators and its effect on searching efficiency. *J.*
498 *Anim. Ecol.* 44, 331–340. <http://www.jstor.org/stable/3866>

499 Beltrami E. and Carroll T.O. (1994). Modeling the role of viral disease in recurrent phytoplankton blooms. *Journal*
500 *of Mathematical Biology* 32: 857-863. <https://link.springer.com/article/10.1007/BF00168802>

501 DeAngelis D., Goldstein R., O’Neill R. (1975). A model for tropic interaction. *Ecology* 56, 881–892.
502 <http://www.jstor.org/stable/1936298>

503 Cantrell R. S., Cosner C., & Ruan S. (2004). Intraspecific interference and consumer-resource dynamics. *Discrete*
504 *and continuous dynamical systems series b*, 4, 527-546. <https://doi.org/10.3934/dcdsb.2004.4.527>

505 Clark R. E., Basu S., Lee B. W., and Crowder D. W. (2019). Tri-trophic interactions mediate the spread of a vector-
506 borne plant pathogen. *Ecology* 100(11): e02879. <https://doi.org/10.1002/ecy.2879>

507 Cohen J., Briand F., Newman C. and Palka Z.J. (1990). *Community Food Webs: Data and Theory.* (Biomathemat-
508 ics). Springer, Berlin, 308p. <https://doi.org/10.1007/978-3-642-83784-5>

509 Crowder D. W., Li J., Borer E.T., Finke D.L., Sharon R., Pattemore D.E. and Medlock J. (2019). Species interactions
510 affect the spread of vector-borne plant pathogens independent of transmission mode. *Ecology* 100: e02782.
511 <https://doi.org/10.1002/ecy.2782>

512 Cuff J.P., Windsor F.M., Terce! M.P.T.G., Bell J.R., Symondson W.O.C., and Vaughan I.P. (2023). Temporal varia-
513 tion in spider trophic interactions is explained by the influence of weather on prey communities, web build-
514 ing and prey choice. *Ecography*: e06737. <https://doi.org/10.1111/ecog.06737>

515 Dobson A.K., Lafferty K.F., Kuris A., Hechinger R., and Jetz W. (2008). Hommage to Linnaeus: How many para-
516 sites? How many hosts? *PNAS* 105:114 82–11489. <https://doi.org/10.1073/pnas.0803232105>

517 Dornelas M., Gotelli N.J., McGill B., Shimadzu H., Moyes F., Sievers C., Magurran A.E. (2014). Assemblage time
518 series reveal biodiversity change but not systematic loss. *Science*. 344, 296-9.
519 <https://www.science.org/doi/10.1126/science.1248484>

520 Douine M., Gozlan R.E., Nacher M., Dufour J., Reynaud Y., Elguero E., Combe M., Velvin C.J., Chevillon C., Berlioz-
521 Arthaud A., Labbé S., Sainte-Marie D., Guégan J.-F., Pradinaud R. and Couppié P. (2017). *Mycobacterium*
522 *ulcerans* infection (Buruli ulcer) in French Guiana, South America, 1969-2013: an epidemiological study.
523 *Lancet Planetary Health* 1: e65-73. [https://doi.org/10.1016/S2542-5196\(17\)30009-8](https://doi.org/10.1016/S2542-5196(17)30009-8)

524 Finke D. L. (2012). Contrasting the consumptive and non-consumptive cascading effects of natural enemies on
525 vectorborne pathogens. *Entomologia Experimentalis et Applicata* 144: 45-55. [https://doi.org/10.1111/j.1570-](https://doi.org/10.1111/j.1570-7458.2012.01258.x)
526 [7458.2012.01258.x](https://doi.org/10.1111/j.1570-7458.2012.01258.x)

527 Frainer A., McKie B. G., Amundsen P.-A., Knudsen R. and Lafferty, K. D. (2018). Parasitism and the biodiversity-
528 functioning relationship. *Trends Ecol. Evol.* 33, 260–268 (2018). <https://doi.org/10.1016/j.tree.2018.01.011>

529 Ghanbari B. & Kumar D. (2019). Numerical solution of predator-prey model with Beddington-DeAngelis
530 functional response and fractional derivatives with Mittag-Leffler kernel. *Chaos: An Interdisciplinary Journal of*
531 *Nonlinear Science*, 29(6). <https://doi.org/10.1063/1.5094546>

532 Garchitorena A., Ngonghala C.N., Landier J., Texier G., Landier J., Eyangoh S., Bonds M., Guégan J.-F. and Roche B.
533 (2015a). Environmental transmission of *Mycobacterium ulcerans* drives dynamics of Buruli ulcer in endemic
534 regions of Cameroon. (Nature) *Scientific Reports* 5: 18055. <https://doi.org/10.1038/srep18055>

535 Garchitorena A., Guégan J.-F., Léger L., Eyangoh S., Marsollier L., and Roche B. (2015b). *Mycobacterium ulcerans*
536 dynamics in aquatic ecosystems are driven by a complex interplay of abiotic and biotic factors. *eLife* 4: e07616.
537 <https://doi.org/10.7554/eLife.07616>

538 Godfray H. C. J., Briggs C. J., Barlow N. D., O’Callaghan M., Glare T. R. and Jackson T. A. (1999). A model of insect-
539 pathogen dynamics in which a pathogenic bacterium can also reproduce saprophytically. *Proc. Royal Society B:*
540 *Biol. Sci.*, 266(1416), 233-240. <https://doi.org/10.1098/rspb.1999.0627>

541 Guégan J.-F., Ayouba A., Cappelle J. and Thoisy B. de (2020). Emerging infectious diseases and tropical forests:
542 unleashing the beast within. *Environmental Research Letters* 15 083007.
543 <https://iopscience.iop.org/article/10.1088/1748-9326/ab8dd7/pdf>

- 544 Guerra C.A., Delgado-Baquerizo M., Duarte E., Marigliano O., Gørgen C., Maestre F.T. and Eisenhauer N. (2021).
545 Global projections of the soil microbiome in the Anthropocene. *Global Ecol Biogeogr* 2021: 30: 987-99.
546 <https://doi.org/10.1111/geb.13273>
- 547 Ji J. and Wang L. (2022). Competitive exclusion and coexistence in an intraguild predation model with
548 Beddington–DeAngelis functional response. *Communications in Nonlinear Science and Numerical Simulation*,
549 107, 106192. <https://doi.org/10.1016/j.cnsns.2021.106192>
- 550 Johnson P.T.J., de Rooode J.C. and Fenton A. (2015). Why infectious disease research needs community ecology?
551 *Science* 349: 1259504. <https://doi.org/10.1126/science.1259504>
- 552 Kuris A.M., Lafferty K.D. and Sokolow S.H. (2014). Saprozonosis: a distinctive type of infectious agent. *Trends*
553 *Parasitol* 30: 386-393. <https://doi.org/10.1016/j.pt.2014.06.006>
- 554 Lafferty K.D., Allesina S., Arim M., Briggs C.J., De Leo G., Dobson A.P., Dunne J.A., Johnson P.T.J., Kuris A.M.,
555 Marcogliese D.J., Martinez N.D., Memmott J., Marquet P.A., McLaughlin J.P., Mordecai E.A., Pascual M., Poulin
556 R. and Thielges D.W. (2008). Parasites in food webs: the ultimate missing links. *Ecology Letters* 11: 533-546.
557 <https://doi.org/10.1111/j.1461-0248.2008.01174x>
- 558 Lanzas C, Davies K, Erwin S and Dawson D. (2020). On modelling environmentally transmitted pathogens. *Royal*
559 *Society Interface Focus*. <https://doi.org/10.1098/rsfs.2019.0056>
- 560 Morris A., Guégan J.-F., Andreou D., Marsollier L., Carolan K., Le Croller M., Sanhueza D. and Gozlan R.E. (2016a).
561 Deforestation-driven food web collapse linked to emerging tropical disease, *Mycobacterium ulcerans*. *Science*
562 *Advances* 2: e1600387. <https://www.science.org/doi/10.1126/sciadv.1600387>
- 563 Morris A., Guégan J.-F., Benbow M.E., Williamson H., Small P.L.C., Quaye C., Boakye D., Merritt R.W. and Gozlan
564 R.E. (2016b). Functional diversity as a new framework for understanding the ecology of an emerging
565 generalist pathogen. *EcoHealth* 13: 570-581. <https://doi.org/10.1007/s10393-016-1140-x>
- 566 Ostfeld R.S., Keesing F. and Eviner V.T. (2008). *Infectious Disease Ecology. The Effects of Ecosystems on Disease*
567 *and of Disease on Ecosystems*. Princeton University Press, Princeton, NJ, 506p.
568 <https://www.jstor.org/stable/j.ctt7sgg4>
- 569 Receveur J.P., Bauer A., Pechal J.L., Picq S., Dogbe M., Jordan H.R., Rakestraw A., Fast K., Sandel M., Chevillon C.,
570 Guégan J.-F., Wallace J. R., Benbow M. E. (2022). A need for null models in understanding disease
571 transmission: the example of *Mycobacterium ulcerans* (Buruli ulcer disease). *FEMS Microbiol Rev* 46: fuab045.
572 <https://doi.org/10.1093/femsre/fuab045>
- 573 Roche B., Benbow M.E., Merritt R., Kimbiraskas R., McIntosh M., Small P.L.C., Williamson H. and Guégan J.-F.
574 (2013). Identifying the Achilles' heel of multi-host pathogens: The concept of keystone "host" species illus-
575 trated by *Mycobacterium ulcerans* transmission. *Environmental Research Letters* 8: 045009.
576 <https://iopscience.iop.org/article/10.1088/1748-9326/8/4/045009>
- 577 Rohr J.R., Civitello D.J., Halliday F.W., Hudson P.J., Lafferty K.D., Wood C.L., Mordecai E.A. (2020). Towards com-
578 mon ground in the biodiversity-disease debate. *Nat Ecol Evol.* 2020 Jan;4(1):24-33.
579 <https://doi.org/10.1038/s41559-019-1060-6>
- 580 Rossberg A.G. (2013). *Food webs and Biodiversity*. John Wiley and Sons, Chichester, UK, 376p.
581 <https://onlinelibrary.wiley.com/doi/book/10.1002/9781118502181>
- 582 Rossi A., Lisa F., Rubini L., Zappavigna A. and Venturino E. (2014). A food chain ecoepidemic model: infection at
583 the bottom trophic level. *Ecological Complexity*. <https://doi.org/10.1016/j.ecocom.2014.03.003>
- 584 Selakovic S., de Ruiter P.C., and Heesterbeek H. (2014). Infectious disease agents mediate interaction in food
585 webs and ecosystems. *Proceedings of the Royal Society B, London* 281: 20132709.
586 <https://dx.doi.org/10.1098/rspb.2013.2709>
- 587 Sylla A., Chevillon C., Djidjiou-Demasse R., Seydi O., Campos C. A. V., Dogbe M., Fast K. M., Pechal J. L., Rakestraw
588 A., Scott M. E., Sandel M. W., Benbow M. E. and Guégan J. F. (2023). Understanding the Transmission of Bac-
589 terial Agents of Saprozonotic Diseases in Aquatic Ecosystems: A First Spatially Realistic Metacommunity Model.
590 <https://doi.org/10.20944/preprints202312.0764.v1>
- 591 Sylla A., Campos C. A. V., Dogbe M., Fast K. M., Pechal J. L., Rakestraw A., Scott M. E., Sandel M. W., Benbow M.
592 E. and Guégan J. F. (2024a). Script and codes. Zenodo. <https://doi.org/10.5281/zenodo.11085318>

593 Sylla A., Campos C. A. V., Dogbe M., Fast K. M., Pechal J. L., Rakestraw A., Scott M. E., Sandel M. W., Benbow M.
594 E. and Guégan J. F. (2024b). Supplementary Figures. Zenodo. <https://doi.org/10.5281/zenodo.11083413>
595 Tripathi J. P., Abbas S. and Thakur M. (2015). Dynamical analysis of a prey–predator model with Beddington–
596 DeAngelis type function response incorporating a prey refuge. *Nonlinear Dynamics*, 80, 177-196.
597 <https://doi.org/10.1007/s11071-014-1859-2>